New Zealand Journal of Marine and Freshwater Research, 1995: Vol. 29: 589–602
0028–8330/95/2904–0589 $2.50/0

Optical properties of the coastal and oceanic waters off South Island, New Zealand: regional variation

CLIVE HOWARD-WILLIAMS
National Institute of Water and Atmospheric Research Ltd
P. O. Box 8602
Christchurch, New Zealand

ROB DAVIES-COLLEY
National Institute of Water and Atmospheric Research Ltd
P. O. Box 11–115
Hamilton, New Zealand

WARWICK F. VINCENT
Département de Biologie
Université Laval
Québec G1K 7P4, Canada

Abstract A study of the optical properties of the varied water masses in inshore and oceanic waters around the South Island of New Zealand was made. This was a contribution to a larger effort to model the productivity of the southern sector of New Zealand's Exclusive Economic Zone. A combination of spectroradiometry, PAR sensor deployments, transmissometry, and yellow-substance measurement was used at 30 stations to characterise the optical properties of the region. The waters were classified according to Jerlov's system for ocean waters. Inshore sites on the west and east coasts and Foveaux Strait fell into optical types *Coastal I* and *Oceanic III*. *Oceanic II* waters occurred in the Subtropical Convergence Zone (STCZ). Subantarctic waters and those south of the STCZ were in the clear categories *Oceanic I* and *IB*. Attenuation coefficients (K) varied more than three-fold from 0.05 to 0.16 m^{-1}. Reflectance was lowest off the Fiordland coast where light-absorbing yellow substance was maximal. An index of the average lighting of the mixed layer ($\overline{E}_o$) for phytoplankton photosynthesis was calculated from the light-depth profile. Highly varying mixed-layer depths, combined with a 3-fold difference in K, caused $\overline{E}_o$ to vary by as much as 11, suggesting that the growth of oceanic phytoplankton in the region may vary far more than predicted by present models.

Keywords absorption; scattering; light climate; spectral attenuation; reflectance; mixed layer

INTRODUCTION

The waters off the South Island of New Zealand (spanning latitudes 40–50°S) display a high degree of physical variability induced by boundary currents, upwelling, and other phenomena (Heath 1976, 1985) and a range of incident solar radiation. The variability of these factors in combination, create a diversity of conditions for ocean planktonic communities. Coastal Zone Colour Scanner (CZCS) satellite images of phytoplankton concentrations over the Southern Ocean show a five-fold variation in mean summer chlorophyll concentrations around the South Island (Sullivan et al. 1993). Synoptic water column sampling and satellite sea surface temperature imagery used by Vincent et al. (1991) similarly testify to the environmental variability in this region. This latter work emphasised the strong north-south and east-west gradients in the oceanic environment, with related spatial patterns between nutrients and temperature, and a strong influence of freshwater inputs around the coast. Large site-to-site differences were detected in fluorescence yield of phytoplankton per unit of chlorophyll *a* concentration. That study also showed the depth of the mixed layer to vary widely with location, such that surface chlorophyll *a* concentrations (mg m^{-3}) were only weakly related to total water column chlorophyll (mg m^{-2}) and, presumably, to depth-integrated productivity.

Vincent, Wake et al. (1989) developed a simple model to examine the influence of temperature and irradiance on daily primary production as a function

M95026
Received 27 April 1995; accepted 28 September 1995

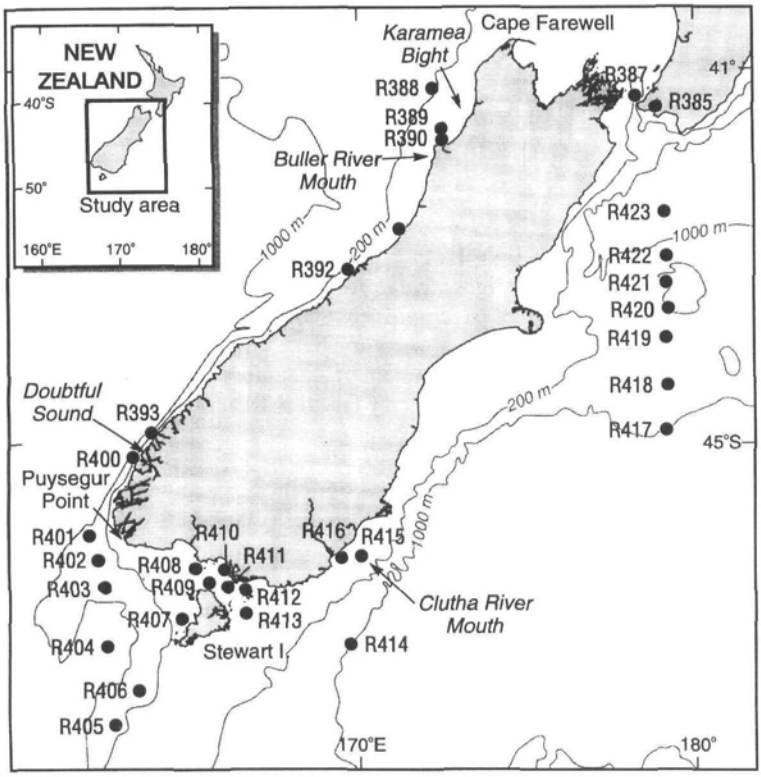

Fig. 1 Map of the South Island of New Zealand showing marine stations sampled on Voyage 2027 of RV *Rapuhia* (16–28 May 1989).

of latitude in the oceanic waters of New Zealand's Exclusive Economic Zone. A central parameter in the irradiance equations in the model was the diffuse attenuation coefficient for irradiance (K), which was assumed to take a single value ($K = 0.07$ m^{-1}) across all water masses. However there are reasons for expecting appreciable variation in K (Vincent et al. 1991; Davies-Colley 1992). The varied biological communities and chlorophyll *a* concentrations in the oceanic waters around the South Island, together with suspended matter and dissolved organic matter from rivers, all affect the underwater light field offshore.

The aim of this study was to provide the first detailed report on optical properties for the diverse range of waters around the South Island. We conducted depth-profile measurements in a range of contrasting water masses which included: inshore waters influenced by land run-off and fiordic exchanges, the West Coast upwelling area, the Sub-Tropical Convergence Zone (STCZ), sub-antarctic waters, Foveaux Strait, and Cook Strait. Here we examine the correlations between the optical properties and other biological and physical characteristics of the waters, and classify the water masses according to Jerlov's optical classification (Jerlov 1951, 1976). The optical data presented here will aid the early interpretation of optical imagery (e.g., SeaWiFS) of the ocean around New Zealand. The work is a contribution to the goal of modelling productivity of New Zealand's Exclusive Economic Zone.

METHODS

All measurements were conducted during voyage 2027 of RV *Rapuhia* between 16 and 29 May 1989. The voyage track encircled the South Island (Fig. 1) and included seven stations off the South Island west coast, five south-west of the South Island, six through Foveaux Strait (between the South Island and Stewart Island), and seven across the Chatham Rise on the eastern side of the South Island, as well as additional stations to sample specific coastal (e.g., river plumes) and oceanographic features (e.g., Subtropical Convergence).

For conductivity and temperature profiling, a Guildline Model 8755 Conductivity-Temperature-Depth instrument was used, mounted on the rosette sampler. The thermistor was calibrated immediately after the cruise with a PRT bridge (Automatic Systems Laboratories Model F6). Salinity samples were subsequently measured with a Guildline Autosal Laboratory Salinometer, Model 8400A. The absolute error in the CTD measurements after calibration correction is estimated as less than ± 0.025 psu (practical salinity units), ± 0.010°C (temperature), and ± 1 m depth.

Chlorophyll *a* fluorescence was profiled with a Seamartek in situ fluorometer that was shielded from ambient light and mounted at the same level as the CTD on the rosette sampler. For absolute measurements of chlorophyll *a*, duplicate one-litre samples from each depth sampled for nutrients were filtered on to 4.25 cm (diameter of filter clearing area) Whatman GF/F filters and stored frozen. Subsequently the filters were ground with 90% acetone in a Teflon tissue grinder, the extract was cleared by centrifugation, and then assayed for chlorophyll *a* by fluorometry both before and after acidification (Strickland & Parsons 1972). Calibration of the Aminco spectrofluorometer was carried out using standard pure chlorophyll *a* (Sigma Chemical Inc.) in acetone.

Duplicate samples for particulate nitrogen and phosphorus analysis were filtered through acid-washed, precombusted Whatman GF/F filters. These were subsequently Kjeldahl-digested and measured by auto-analyser as described in Vincent, Chang et al. (1989). The filtrates were analysed immediately for dissolved nutrients (nitrate plus nitrite, ammoniacal-N, urea) or were stored frozen for up to 2 months before analysis (silica, dissolved reactive phosphorus), using the auto-analytical methods detailed in Vincent, Chang et al. (1989).

Yellow substance was measured on samples collected from 10 m depth by absorption at 440 nm of 0.22 µm filtered (Sartorius membrane filters) samples in 40 mm matched cuvettes in a PU8800 Pye-Unicam spectrophotometer (Bricaud et al. 1981; Davies-Colley 1992). The reference was pre-filtered high-quality double glass-distilled water.

Symbols and units of the measured optical properties are given in Table 1. The shipboard procedure for all measurements was as follows: the ship was manoeuvred so that the sun was on the side where the measurements were to be taken. The instruments were lowered from a crane stretched out 10 m from the ship's side. Three instruments were deployed, a Photosynthetically Available Radiation (PAR) sensor array, a spectroradiometer, and a transmissometer. The PAR

Table 1 Symbols and units referred to in the text. Beam attenuation (1) was measured directly with the Martek transomissometer, beam attenuation (2) was calculated from $a + b$ derived from PAR data.

Variable	Symbol	Unit
Scalar irradiance (1) 400–700 mm	E_o	µmol m^{-2} s^{-1}
Downward irradiance 400–700 nm	E_d	µmol m^{-2} s^{-1}
Upward irradiance 400–700 nm	E_u	µmol m^{-2} s^{-1}
Downward spectral irradiance 5 nm intervals 350–750 nm	$E_d(\lambda)$	W m^{-2} nm^{-1}
Upward spectral irradiance 350–750 nm	$E_u(\lambda)$	W m^{-2} nm^{-1}
Sea state	Sea	Dimensionless
Cloud cover	Cloud	/8
Attenuation coefficient for scalar irradiance	K_o	m^{-1}
Attenuation coefficient for downward irradiance	K_d	m^{-1}
Attenuation coefficient for upward irradiance	K_u	m^{-1}
Euphotic depth	z_{eu}	m
Reflectance (400–700 nm)	R	Dimensionless
Average cosine (at the midpoint of the Euphotic zone)	µ	Dimensionless
Absorption coefficient (400–700 nm)	a	m^{-1}
Scattering coefficient (400–700 nm)	b	m^{-1}
Beam attenuation (1)	$c(530)$	m^{-1}
Beam attenuation (2)	c	m^{-1}
Spectral attenuation coefficient for downward irradiance	$K_d(\lambda)$	m^{-1}
Spectral reflectance	$R(\lambda)$	Dimensionless
Sun angle	Sun	
Angle of the solar beam	90–ß	

instrument array consisted of a Licor Scalar Irradiance probe (Model LI 193 SB) and two Licor cosine response probes (Model LI 192): one facing up and one down, to provide almost simultaneous readings of E_o, E_d, and E_u.

Downward and upward facing deployments of the LiCor 1800UW scanning spectroradiometer were made consecutively. Efforts were made to ensure that irradiance spectra were not distorted by changes in ambient irradiance during scanning. The transmissometer was a Martek XMS with a 0.25 m path and a filter peak wavelength of 530 nm. (A 1 m path length instrument would have been preferable for clear ocean water but was not available at the time.) A LiCor LI–1000 data logger continuously recorded solar radiation in the waveband 400–700 nm (using a LiCor LI–190SA quantum irradiance sensor).

Attenuation coefficients for the downwelling vector irradiance (K_d) and for scalar irradiance (K_o) were calculated from the slope of the linear regression of the natural log-transformed irradiance measurements versus depth. The euphotic depth (depth to 1% of surface light level) was estimated as $4.6/K_d$. Reflectance (E_u/E_d) and the average cosine (μ) (Kirk 1981) were used to compute the PAR band averaged absorption coefficient and scattering coefficients according to Kirk's (1981) method. Spectral attenuation coefficients ($K_d(\lambda)$) were calculated from:

$$K_d(\lambda) = \ln [E_d(\lambda,z)/E_d(\lambda,z + \Delta z)] / \Delta z \quad (1)$$

for the depth interval Δz. $K_u(\lambda)$ was calculated from the equivalent equation for E_u.

Spectral Reflectance $R(\lambda)$ was calculated from

$$R(\lambda) = E_u(\lambda)/E_d(\lambda). \quad (2)$$

PAR-band integrations of the spectral irradiance were used to check that the spectral irradiances appearing in Eq. 1 and 2 had not been obtained under different lighting conditions.

Table 2 Weather conditions and sea state at all stations. Units and symbols are: Cloud, visually estimated in octets; Sea, visually assessed on Beaufort scale; Sun, sun angle, degrees calculated from time (NZST) and 40° latitude nomograms of Walker & Trexler (1977) with corrections for latitude at each station; 90–ß, angle incident of the direct solar beam where ß is solar altitude (90–ß = 43 under occluded sun, OC).

Station	Site	Date	Time	Cloud	Sun	90–ß	Sea	Notes
387	Narrows	16 May 89	15.15	3/8	20	70	1	
388	Outer Westport Line	17 May 89	14.30	7/8	OC/26	43/64	4	Patchy cloud
389	Mid-shelf, Westport Line	17 May 89	20.30	Night	Night	Night	–	Night
390	Inshore, Westport Line	17 May 89	22.00	Night	Night	Night	–	Night
391	Hokitika inshore	18 May 89	08.30	0/8	8–13	77–82	2	
392	Abut Head	18 May 89	15.15	0/8	20	70	1?	
393	Off Thompson Sound	19 May 89	11.25	8/8	OC	43	5–6	
400	Off Doubtful Sound	21 May 89	15.00	7/8	OC	43	5–6	
401	Puysegur Point	22 May 89	09.00	7/8	OC	43	2–3	
402	Puysegur/Snares Track	22 May 89	14.15	5/8	24	66	2–3	
403	Puysegur/Snares Track	22 May 89	16.35	6/8	10	80	3	
404	Puysegur/Snares Track	22 May 89	22.00	Night	Night	Night	2–3	Night
405	Snares	23 May 89	09.50	0/8	13	77	3–4	
406	Stewart Island Track	23 May 89	15.05	8/8	OC	43	3	
407	Stewart Island Track	23 May 89	22.30	Night	Night	–	–	Night
408	Stewart Island Track	24 May 89	08.45	8/8	OC	43	4	
409	Foveaux Strait	24 May 89	11.40	8/8	OC	43	4–5	
410	Foveaux Strait	24 May 89	13.20	8/8	OC	43	6	
411	Foveaux Strait	24 May 89	15.00	8/8	OC	43	3–4	
412	Foveaux Strait	24 May 89	17.30	Night	Night	Night	2–3	Night
413	Foveaux Strait	24 May 89	19.30	Night	Night	Night	–	Night
414	Sub–antarctic zone	25 May 89	09.00	0/8	7	83	3	
415	Clutha offshore	25 May 89	16.20	0/8 haz	8	82	5	Stratified water
416	Clutha inshore	25 May 89	19.00	Night	Night	Night	–	Night
417	Chatham Rise South	26 May 89	21.00	Night	Night	Night	7–8	Night
418	Chatham Rise	27 May 89	08.30	5–6/8	OC	43	7	Variable light
419	Chatham Rise	27 May 89	13.00	5–6/8	OC/28	43/62	7	Variable light
420	Chatham Rise	27 May 89	17.40	Night	Night	Night	–	Night
421	Chatham Rise	28 May 89	08.10	5–6/8	OC	43	6	Patchy cloud
422	Chatham Rise	28 May 89	12.30	5/cirrus	29	61	4–6	Patchy cloud

The depth of the mixed layer (Z_m) was defined from the first major density discontinuity detected in the CTD profiles, and the average lighting over the mixed layer was estimated from the average quantum scalar light intensity for the mixed layer $\overline{E}_o$ defined as:

$$\overline{E}_o = \frac{1}{Z_m} \int_{0_m}^{z_m} E_o(z)dz \quad (3)$$

which can be simplified (Vincent 1983) to:

$$\overline{E}_o = E_o(0)/(K_o Z_m) \quad (4)$$

RESULTS

Sea, weather, and solar conditions at the time of sampling are given in Table 2.

Water masses

The water masses encountered on this cruise have been grouped by Vincent et al. (1991) into the following types on the basis of their origins, temperatures, salinities, and other properties: inshore coastal, West Coast oceanic, subtropical convergence, sub-antarctic. Table 3 gives data on temperature, salinity, mixed depth, chlorophyll *a*, g_{440} and PN for stations so grouped.

Inshore/coastal

This includes inshore west coast, inshore east coast, and Foveaux Strait (Table 3). Mixed-layer depths were generally shallow (< 40 m) and salinity and temperature comparatively variable as might be expected. Moderate chlorophyll *a* concentrations were found, varying between 0.26 and 0.71 mg m^{-3}.

Table 3 Temperature, salinity, mixed layer depths (Z_m), chlorophyll *a*, yellow substance (g_{440}), and an index of particulate matter (PN) at all sites; analyses from 10 m depth. STCZ, Subtropical convergence zone.

Region (type)	Station	Temp. (°C)	Salinity (psu)	Z_m (m)	Chl. *a* (mg m^{-3})	g_{440} (m^{-1})	PN (mg m^{-3})
Inshore/coastal (west)	390	14.60	34.62	36	0.41	0.090	1.01
	391	14.49	34.31	35	0.71	0.040	0.97
	393	14.56	34.09	25	0.53	0.083	1.07
	400	14.17	34.28	10†	0.52	0.109	1.11
	415	11.17	33.79	10†	0.29	0.058	1.06
Inshore/coastal (east)	416	11.37	33.90	10†	0.62	0.060	1.41
	409	12.47	34.76	48	0.38		0.64
Foveaux Strait	410	11.96	34.54	28	0.34		0.43
	411	12.14	34.70	34	0.26		0.52
	412	11.95	34.62	23	2.29	0.052	0.52
	413	11.61	34.72	55	0.33		0.72
West Coast	387	15.41	34.92	35	0.30	0.085	0.91
	388	15.72	34.85	45	0.29	0.070	0.78
	389	15.19	34.61		0.43	0.064	0.76
	392	14.94	34.68	30†	0.70	0.042	0.92
STCZ:							
South-western oceanic	401	13.73	34.89	95	0.32	0.049	0.58
	402	13.82	34.88	95	0.46	0.023	0.91
	403	13.13	34.92	95	0.42	0.045	0.61
	404	12.37	34.82	120	0.24	0.062	0.50
	405	11.97	34.77	198	0.17	0.091	0.42
	406	12.04	34.77	110	0.22		0.38
	407	13.22	34.89	80	0.14		0.48
	408	12.98	34.82	52	0.47	0.102	1.10
STCZ:							
Chatham Rise	418	9.82	34.34	60	0.30	0.014	0.72
	419	11.73	34.51	55	1.46	0.030	1.15
	420	13.08	34.72	100	0.51	0.022	0.74
	421	13.05	34.71	100	0.27	0.085	0.06
	422	12.74	34.63	70	0.62	0.034	0.77
Sub-antarctic	414	9.5	34.36	100	0.22	0.027	0.65
	417	9.73	34.25	60	0.24	0.031	0.85

†complex structure

Levels of yellow substance were relatively high with g_{440} ranging from 0.04 to 0.11 m^{-1}.

West Coast

Water temperatures were warm (14.9–15.7°C), salinities varied little (34.61 and 34.92 psu), and mixed-layer depths were shallow (30–45 m: Table 3). Yellow substance level as g_{440} varied between 0.04 and 0.085 m^{-1}, and chlorophyll *a* concentration was low to moderate (0.29–0.7 mg m^{-3}).

Subtropical convergence

(i) South-western oceanic

Temperatures ranged from 12.37°C at the south (Snares Island) to 13.82° at the north with a narrow salinity range in the surface waters (34.77–34.92 psu). Deep mixed layers (> 90 m) were a feature of these waters. g_{440} levels were low and ranged between 0.023 and 0.062 m^{-1}. Chlorophyll *a* concentration was low, always less than 0.5 mg m^{-3} (Table 3).

(ii) Chatham Rise

Mixed-layer depths varied from 55 to 100 m with the shallowest mixed layer near the top of the Chatham Rise. Temperatures increased from south to north: 9.7° at Stn 417 (latitude 45°00'S) to 13.08° on the R:ise itself (latitude 43°19.9'). Slightly cooler waters (c. 12°C) were recorded north of the rise associated with the large eddies identified in Vincent et al. (1991). Chlorophyll *a* concentration was highly variable with low values (0.3 mg m^{-3} or less) south of the Rise and higher values (up to 1.46 mg m^{-3}) on the Rise and to the north. Yellow substance level was low (< 0.04 m^{-1}) at all sites throughout the transect, except Stn 421 to the north of the Rise.

Sub-antarctic waters

These are represented by Stn 414 (Fig. 1) and Stn 417. The temperature at Stn 414 was 9.5°, salinity was low (34.36 psu), and nutrient concentrations were high compared with elsewhere (Table 3). These waters were low in chlorophyll *a* content (0.22 mg m^{-3}) in spite of being nutrient-rich. Yellow substance level was low (< 0.03 m^{-1}).

Optical properties

Irradiance attenuation coefficients (K) were generally higher off the west coast than off the east coast (Table 4). The clearest waters were those of the sub-antarctic water mass (e.g., Stn 414 with K_0 = 0.05 m^{-1}, and a corresponding euphotic zone of 104 m).

Table 4 Selected optical properties in the PAR wave band at the major water masses of the South Island.

Water mass	Station	K_d (m^{-1})	K_o (m^{-1})	Z_{eu} (m)	$\overline{E}_o$ (%)	R (%)	a (m^{-1})	b (m^{-1})	c (m^{-1})	c (530) (m^{-1})
Inshore/coastal	391		0.158	25	18.1	3.4	0.098	0.312	0.411	0.475
	393	0.140	0.139	33	28.8	1.6	0.101	0.181	0.282	0.364
	400	0.166	0.159	28	62.9	2.2	0.114	0.298	0.412	0.557
	409		0.079	58	26.3					0.239
	410		0.115	40	31.1					0.338
	411	0.122	0.126	38	23.3	3.8	0.078	0.312	0.390	
	415		0.108	43	92.6	4.2	0.064	0.266	0.330	
West Coast	387		0.104	45	27.5					
	392	0.144	0.144	32	23.2	3.3	0.086	0.294	0.380	0.520
STCZ: South-western oceanic	401	0.084		55		2.8	0.056	0.168	0.224	0.368
	402	0.099	0.094	47	11.2	3.0	0.061	0.190	0.251	0.350
	403		0.067	66	15.7	2.0	0.053	0.101	0.168	
	405	0.068	0.064	70	7.9	3.3	0.042	0.135	0.177	0.151
	406		0.067	66	13.6					
	408	0.106	0.092	43	20.9	2.1	0.073	0.183	0.256	0.364
STCZ: Chatham Rise	418	0.065		68	26.0	4.1	0.041	0.177	0.217	0.282
	419	0.112	0.121	41	15.0	3.1	0.072	0.229	0.301	0.360
	421		0.059	78	16.9					0.274
	422	0.103	0.094	54	15.2	3.4	0.066	0.217	0.283	0.377
Sub-antarctic	414	0.048	0.050	104	20.0	4.0	0.033	0.113	0.148	0.083

The attenuation coefficients varied more than threefold from 0.05 to 0.17 m^{-1}. As expected the inshore coastal waters generally had the highest K_d but the offshore waters also included some high values among a wide variation in K_d.

Inherent optical properties shown in Table 4 are the PAR band average absorption coefficient (a), the scattering coefficient (b), and beam attenuation coefficient (c).

Maximum values of a and b and c were found at the inshore coastal stations as would be expected. For oceanic waters, values of a were greater off the west coast than on the east side of the South Island. The lowest values were recorded at Stn 405 (0.042 m^{-1}), 418 (0.040 m^{-1}), and 414 (0.030 m^{-1}) in sub-antarctic waters. No data were available for Stn 417 (sampled at night, Table 2) which, also being a cold "sub-antarctic" water, is expected to be clear. Lowest scattering coefficients ($b < 0.14$ m^{-1}) and beam attenuation coefficients ($c < 0.18$ m^{-1}) were at the southernmost stations where recordings were made (Stn 403, 405, 414).

The ratio of scattering to absorption, b/a, which correlates closely with reflectance (e.g., Kirk 1994), was near constant in the range 3.1–4.4 for all stations other than the two inshore stations 393 and 400 on the west coast off Fiordland. Low ratios of 1.8 and 2.6, respectively, were recorded here, owing to the relatively high levels of yellow substance and its consequent influence on the absorption coefficient (Tables 3, 4).

Spectral characteristics

The various water masses could be distinguished by their spectral attenuation properties. This is illustrated in Fig. 2A by the $K_d(\lambda)$ plots for four representative stations in contrasting waters: Stn 391, West Coast; Stn 400, inshore/coastal, West Coast; Stn 414, sub-antarctic; and Stn 422, Chatham Rise. Station 400 showed a relatively high attenuation at the blue end of the spectrum owing to a relatively high yellow-substance concentration ($g_{440} = 0.11$ m^{-1}), with a minimum between 500 and 570 nm, a green "window". The curve for west coast oceanic water (Stn 391) was similar but with lower blue attenuation. Clear waters with a distinct blue-green window (minimum $K_d(\lambda) = 500$ nm) were characteristic of the north Chatham Rise (Stn 422). The sub-antarctic water (Stn 414), with its low attenuation at the blue end of the spectrum and a blue window between 410 and 470 nm was close to optically pure sea water (Smith & Baker 1981).

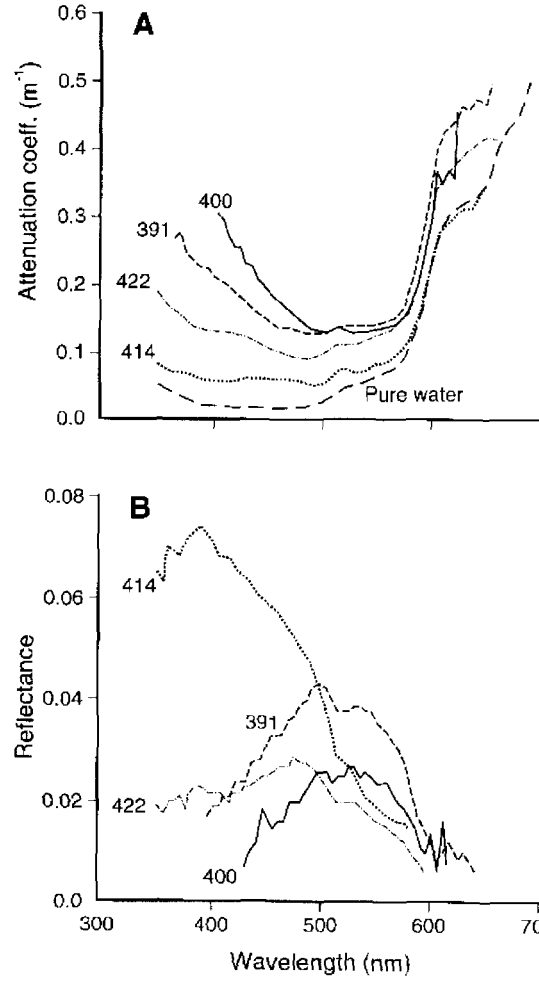

Fig. 2 **A**, Spectral attenuation K_d (λ) values for four contrasting stations. Spectral K for purest ocean waters (after Smith & Baker 1981) is shown for comparison. **B**, Spectral reflectance R (λ) for the same four contrasting stations.

Spectral reflectance ($R(\lambda)$ followed a broadly inverse trend (Fig. 2B) with maximum reflectance at 520 nm for Stn 400, 500 nm for Stn 391, 480 nm for Stn 422, and 400 nm for Stn 414. Most of the off-shore waters showed maximum reflectance in the 450–500 nm range, and appeared blue to green. Sub-antarctic water had maximal reflectance at shorter wavelengths and appeared blue in hue.

Contributions to absorption

The contribution to the total absorption coefficient of yellow substance (a_y), particulate matter (a_p), chlorophyll (a_{chla}), and water itself (a_w) at 440 nm

was estimated. The total absorption coefficient $a(440)$ was calculated from irradiance data where: $a(440) = \mu(440)\ K_d(440)$ (Kirk 1981) and μ was calculated from spectral reflectance, $R(440)$ (Kirk 1981). g_{440} data were used for absorbance by yellow substance at each station, and that due to phytoplankton pigments at 440 nm (a_{chla}) calculated from the method of Bricaud & Stramski (1990) using the lower end of the range of published values for the specific absorption coefficient for phytoplankton (Prieur & Sathyendranath 1981). The values of a_{chla} were obtained by multiplying the absorption correction of $A_{chla} = 15\ m^2\ g^{-1}$ by the measured values of chlorophyll *a* recorded in Table 2. The remainder was attributed to absorption by non-chlorophyll particulate matter a_p, where:

$$a_p = a(440) - (a_w + g + a_{chla})$$

all at 440 nm, where a_w is the absorption due to water itself (Smith & Baker 1981).

Data for a selected range of stations (Table 5) show that the contribution of pure water to the total absorption (i.e. a_w/a) at 440 nm is high in the south-western oceanic (Stn 402) and southern side of the STCZ (Stn 418): 32 and 40%, respectively. The contribution of yellow substance at this wavelength varied between 37 and 66%, but that due to phytoplankton pigments was generally less than 20%. One exception was at Stn 419 in the eddy on the Chatham Rise where 31% of the absorption coefficient at 440 nm was attributable to phytoplankton. Chlorophyll *a* concentrations were used in this calculation for absorption due to phytoplankton. Although chlorophyll *a* is the dominant pigment it is only one pigment in an assemblage of different pigments in the phytoplankton (Hoepffner & Sathyendranath 1992) so chlorophyll *a* alone may underestimate the proportional contribution by phytoplankton. Absorption due to non-living particulate matter was a highly variable contributor to total absorption (negligible up to 39%).

Average irradiance in the mixed layer

The average irradiance that a circulating cell in the mixed layer is subjected to ($\overline{E}_o$), was calculated as a percentage of subsurface irradiance (Table 3) to provide an index of the degree of illumination of the mixed layer. Relatively low values (< 15%) were found in the deep mixed layers of the STCZ (Stn 405, 406). While a deep mixed layer (Z_m = 100 m) occurred in the sub-antarctic Stn 414, the high clarity of this water (Z_{eu} = 104 m) more than compensated, giving a relatively high $\overline{E}_o$ of 20%. A high $\overline{E}_o$ value of 92% at Stn 415 resulted from the very shallow mixed layer (c. 10 m) in this highly stratified coastal water mass, affected by a freshwater plume from the Clutha River.

General correlations between properties

Several significant correlations were observed between optical variables and certain chemical, and biological variables (Table 6). K_o was correlated to chlorophyll *a* ($r = 0.504$, $P < 0.05$), yellow substance ($r = 0.504$, $P < 0.05$), and particulate matter expressed as particulate nitrogen ($r = 0.62$, $P < 0.05$) and was also correlated with water temperature and negatively with distance from land. (Note that K_d was very similar numerically to K_o but good measurements of K_d were available from fewer sites so correlations were made with K_o only.) $\overline{E}_o$ was only weakly related to chlorophyll, yellow substance, or particulate matter, as mixed layer depth was a primary controlling variable on $\overline{E}_o$.

A multiple regression of K_o on chlorophyll *a*, yellow substance, and particulate matter showed

Table 5 Absorption coefficients (m^{-1}) at 440 nm for various components of the water mass. Data in parentheses are the % contribution to total $a(440)$. a_w, absorption by pure water; a_y, absorption due to yellow colour = g_{440}, a_{chla} absorption due to chlorophyll *a*; a_p, absorption due to non-chlorophyll particulate matter.

Station	$a(440)$	a_w	a_y	a_{chla}	a_p
391	0.108	0.014 (13)	0.040 (37)	0.01 (10)	0.043 (39)
400	0.165	0.014 (8)	0.109 (66)	0.008 (5)	0.034 (21)
402	0.043	0.014 (32)	0.023 (53)	0.007 (16)	negl (negl)
418	0.035	0.014 (40)	0.014 (40)	0.004 (11)	0.003 (9)
419	0.070	0.014 (20)	0.030 (43)	0.022 (31)	0.004 (6)
422	0.078	0.014 (18)	0.034 (44)	0.009 (11)	0.021 (27)

the following equations:

For all data:

$$K_o\ m^{-1} = 0.023 + 0.057\ PN + 0.033\ Chl.a + 0.281\ g_{440} \quad (r = 0.71, P < 0.02).$$

For oceanic sites:

$$K_o\ m^{-1} = 0.031 + 0.042\ PN + 0.035\ Chl.a + 0.159\ g_{440} \quad (r = 0.78, P < 0.02).$$

There was a significant correlation between chlorophyll *a* and particulate matter ($r = 0.64$, $P < 0.05$) in the oceanic waters and for the full data set ($r = 0.58$, $P < 0.05$), but removal of particulate matter from the multiple regression equations resulted in a reduced *r*. This was 0.58 ($P < 0.05$) for all sites and 0.69 ($P < 0.05$) for oceanic sites.

There was a moderate correlation ($r = 0.48$, $P < 0.1$) between the absorption coefficient for the PAR waveband and yellow substance, and a stronger correlation between *a* (PAR) with organic particulate matter ($r = 0.64$, $P < 0.01$) suggesting that absorption by non-living particulate matter was more important than by yellow substance for the full PAR waveband in these waters. This arises because yellow substance absorbs mainly in the blue region of the PAR waveband, whereas absorption by particulate matter is less spectrally selective and contributes more attenuation right across the PAR waveband. In the full data set, K_o, *a*, and *c* were negatively related to distance from land, but less strongly when the inshore coastal stations were omitted. There was a positive correlation with temperature as the colder waters of the subantarctic and subtropical convergence were the clearest.

Chatham Rise transect

A highly variable transect across the Chatham Rise is used to illustrate the relationships between the optical parameters. The temperature structure (from Vincent et al. 1991) shown in Fig. 3 revealed a central cell of slightly cooler water in a warm water eddy over the Rise. A sharp temperature gradient to the south of the Rise led to sub-antarctic water. A peak in chlorophyll *a* and particulate matter at Stn 419 was followed by low values in the eddy on the Rise. Beam attenuation and K_o followed this trend, varying by a factor of almost 3. $\overline{E}_o$ fell between Stn 418 and 419, increased only slightly in the clearer waters of the eddy as a result of a deepening of the mixed layer there, and then fell again to the north of the Rise.

DISCUSSION

The negative relationships of K_o, *a*, and *c* to distance from land may arise for two reasons: firstly because land drainage is the source of much light-attenuating matter, and secondly, because nutrients advected into the mixed layer from coastal upwelling (e.g., west coast: Vincent, Chang, et al. 1989; Viner 1990) result in increased planktonic production. This would have consequently increased light attenuation due to increased particulate and dissolved organic matter concentrations.

Table 6 Pearsons correlation coefficients for K_o, *a*, *b*, and *c* against several environmental parameters for the total data set and for oceanic sites only (data are from 10 m samples where appropriate). *, $P < 0.05$; **, $P < 0.01$; ***, $P < 0.001$.

	K_o† (m^{-1})	*a* (m^{-1})	*b* (m^{-1})	*c* (m^{-1})	$\overline{E}_o/E_o(-0)$
All data					
Chlorophyll *a* (mg m^{-3})	0.504*	0.402	0.313	0.356	0.120
Temperature (°C)	0.496*	0.747***	0.375	0.500	0.068
Yellow substance (m^{-1})	0.504*	0.468	0.090	0.192	0.270
Particulate matter (mg PN m^{-3})	0.621**	0.640**	0.428	0.505**	0.390
Distance from land (km)	–0.787***	–0.777***	–0.552*	–0.647**	
n	21	15	15	15	
Oceanic					
Chlorophyll *a* (mg m^{-3})	0.626**	0.641**	0.605*	0.644**	0.048
Temperature (°C)	0.493*	0.767***	0.484	0.582	0.529
Yellow substance (m^{-1})	0.071	0.164	0.155	0.093	0.219
Particulate matter (mg PN m^{-3})	0.582**	0.713***	0.633**	0.676**	0.346
Distance from land (km)	–0.476	–0.481	–0.197	–0.292	
n	16	11	11	11	

†K_d for sites 401 and 418 included

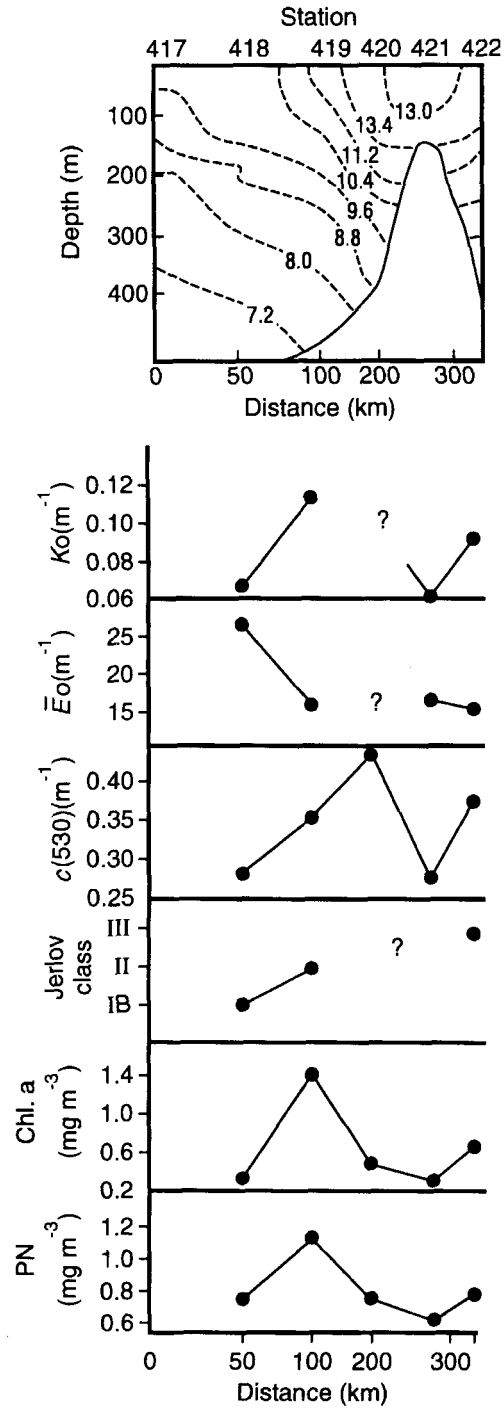

Fig. 3 Transect across the Chatham Rise showing temperature structure, the eddy feature on the Rise, and optical properties across the Rise.

The clearest waters ($K_0 < 0.06$ m^{-1}) were generally found south of the subtropical convergence, where low levels of chlorophyll *a* and yellow substance prevailed. The influence on the optical properties of land-derived material, especially yellow substance, was strikingly evident off the Fiordland coast. Reflectance was lowest at these sites which also shared maximal attenuation $K(\lambda)$ at the blue end of the spectrum. In contrast, the cold, nutrient-rich, but chlorophyll *a*-poor waters of the subantarctic were "blue" (low spectral K and high spectral R in the region 350–450 nm). Large-scale remote sensing analyses of southern ocean biomass (Sullivan et al. 1993) showed that relatively high chlorophyll *a* (> 1.0 mg m^{-1}) could occur in summer in regions occupied by the sub-antarctic water mass.

The data presented in the present paper reflect autumn-winter conditions. A time series of satellite composite images of sea-surface temperatures over the area reveals a regular increase in temperature across and south of the STCZ in summer. Results from a subsequent summer voyage to the STCZ at the Chatham Rise and south to sub-antarctic water (February 1995) show a mixed layer depth of 20–40 m across this area (Singleton 1995). Mixed-layer water temperatures ranged from 18°C in the STCZ to 14°C in subantarctic water. Optical properties in the waters around the South Island in summer time may therefore be appreciably different from those measured in autumn-winter as reported here. In particular the parameter $\bar{E}_o$ may be less variable in summer as a result of surface warming of the ocean and a more-nearly "uniform" shallow mixed-layer depth.

Our data indicate that chlorophyll *a* is a small contributor (< 20%) to the absorption coefficient *a* (Table 5). Kirk's (1981) empirical equation:

$$K_d\,(Z_m) = (a^2 + 0.256\,a\,b)^{1/2}$$

shows that irradiance attenuation is primarily determined by the absorption coefficient. In the open ocean (Stn 401–422) across the STCZ, absorption (and hence K) appears to be dependent on yellow substance and particulate matter, presumably derived from *old* primary production. This would therefore not be expected to co-vary with present chlorophyll *a* values. Fenton et al. (1994) have recently studied optical properties in the surface waters of part of the southern ocean and similarly found that absorption by yellow substance provided a major contribution to K_0.

Optical classification

Jerlov (1951, 1976) provided a scheme for optical classification of ocean waters based primarily on the scattering coefficient (b) and the irradiance attenuation coefficient at 465 nm. This wavelength was assumed to be close to the minimum of the attenuation coefficient for the clearest ocean waters (Jerlov 1951). The widely used Jerlov classification has been modified in recent years by Pelevin & Rutkovskaya (1977) and further refinements have been made by Smith & Baker (1978, 1981). However, these changes have only altered the classification in coastal waters and regions where attenuation is strongly influenced by yellow substance, resuspended sediments, or terrigenous inflows. We have followed Jerlov's classification so as to relate optical character to the autumn-winter physico-chemical patterns around the South Island on the basis of temperature, salinity, and other properties as set out in Table 3. We recognise that the optical classification of surface water at a particular site may vary with season.

The data for K_d (465) and scattering coefficient are given in Table 7 together with the inferred optical type. The inshore/coastal waters all fall into optical types *Coastal 1* and *Oceanic III*. The other extreme is seen by sub-antarctic water at Stn 414 which is in the clearest optical category *Oceanic I*. The only West Coast station where adequate data are available, Stn 392, was classified as *Coastal 1*. This site was off Abut Head only 22 km offshore on the continental shelf. The waters of the sub-tropical convergence south-east of the South Island were clear waters in categories *Oceanic I(B)* and *Oceanic II*. Across the Chatham Rise the clarity increased from north to south with classification *Oceanic III* to the north and *Oceanic I(B)* in the south (Table 7, Fig. 4).

The optical classification is mapped on a broad scale on Fig. 4. Type *Coastal 1* predominated along the West Coast. *Oceanic II* waters occurred in the STCZ to the south of the South Island and on the Chatham Rise. Sub-antarctic waters and those south of the STCZ were types *Oceanic I* and *IB*. Sharp changes across the STCZ at the Chatham Rise show the transition from *Oceanic I(B)* to *Oceanic III* across the Rise.

Prieur & Sathyendranath (1981) pointed out that the classifications of Jerlov (1976) and Smith & Baker (1978) were dependent on an *apparent* property of the water, the attenuation coefficient. They proposed a more rigorous system based on the absorption coefficient, an *inherent* optical property. Their classification was based on the relative importance of three optical coefficients C', Y', and P', expressing the different spectral absorption characteristics of chlorophyll, yellow substance, and non-chlorophyllous particles, respectively. However, in the range of water types covered in this study, the three coefficients are

Table 7 K_d (465), scattering coefficient and Jerlov water types for the major water masses off the South Island.

Water mass	Station	K_d (465) (m^{-1})	b (PAR) (m^{-1})	Jerlov water type
Inshore/coastal	391	0.137	0.312	*Coastal 1*
	393	0.130	0.181	*Coastal 1*
	400	0.168	0.298	*Coastal 1*
	411	0.093	0.312	*Oceanic III*
	415	0.082	0.266	*Oceanic III*
West Coast	392	0.132	0.294	*Coastal 1*
STCZ: South-western oceanic	401	0.065	0.168	*Oceanic II*
	402	0.049	0.190	*Oceanic I(B)*
	403	0.070	0.101	*Oceanic II*
	405	0.050	0.135	*Oceanic I(B)*
	408	0.067	0.183	*Oceanic II*
STCZ: Chatham Rise	418	0.057	0.177	*Oceanic I(B)*
	419	0.069	0.229	*Oceanic II*
	422	0.081	0.217	*Oceanic III*
Sub-antarctic	414	0.035	0.113	*Oceanic I*

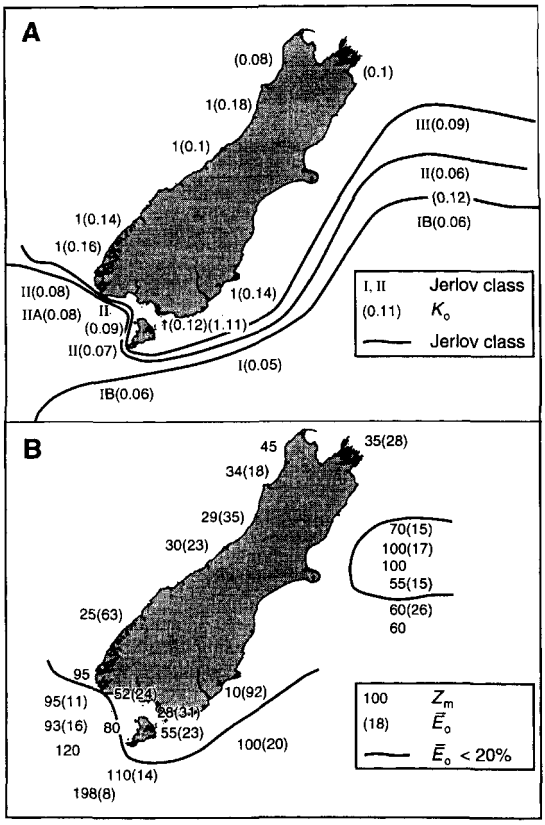

Fig. 4 Map of the sector of the Exclusive Economic Zone where optical measurements were made showing: **A**, the Jerlov classification values, and K_o; and **B**, the mixed-layer depths (Z_m) and average irradiance $\bar{E}_o$ in the mixed layer.

very low (i.e., Jerlov *Oceanic I* and *IA* have negligible coefficients) and hence too imprecisely measured to permit application of this classification.

Applications to models of primary production

For the purposes of modelling ocean primary production and for remote sensing of waters for regional estimations of productivity, *apparent* optical properties K_d (or K_o), R, and the attenuation cross-sections for the constituents affecting the light field (Topliss et al. 1989; Fenton et al. 1994) are used more often than *inherent* properties.

The waters considered in this study span a fairly narrow range of optical types at the high clarity end. In spite of this, K_d (and K_o) varied by as much as 3.5-fold. A model of marine food chain dynamics in a South Island west coast ecosystem (Kumar et al. 1991) was highly sensitive to changes in the light limitation parameter (α) for picoplankton and was also sensitive to changes in K_d. Running the model with a ten-fold change in K_d from 0.07 to 0.7 m^{-1} to a steady state (30 days) resulted in a four- to fivefold decrease in the biomass of picoplankton, nanoplankton, and net plankton components, a fivefold increase in microzooplankton biomass, and a corresponding decrease in macrozooplankton biomass. Evidently light availability strongly influences the West Coast plankton ecology. Kumar et al. (1991) suggested that a shallowing of the mixed layer (Z_m) could partially offset such a decrease in light penetration. Indeed, the average irradiance that a circulating phytoplankton cell is subjected to ($\bar{E}_o$) was consistently higher in the waters with the highest attenuation coefficients (Table 3). In all these waters Z_m was small (c. 30 m or less). Although $\bar{E}_o$ is a valuable indicator of light availability in the mixed layer (e.g., Vincent 1983) the strong non-linearity of production vs irradiance curves precludes direct use of this index in models (McBride 1992).

The significance of the mixed-layer depth in primary production may be affected by photoadaptation by the phytoplankton. For instance the parameters E_k (saturating light intensity) and P_{max} (maximum rate of photosynthesis) are known to be variable (Kirk 1994). Present models of productivity in New Zealand's EEZ have assumed a constant relationship of photosynthesis to irradiance. Studies are currently underway to examine photosynthetic parameters in New Zealand marine waters (I. Hawes, NIWA, pers. comm.).

The EEZ model of Vincent, Wake et al. (1989) showed a three-fold variability in primary production (g C m^{-2} yr^{-1}) from top (latitude 25°S) to bottom (latitude 55°S), primarily owing to variation in incident irradiance and temperature. The model was based on a constant K_d of 0.07 m^{-1} and mixed layer depth was not considered. The present study has shown not only a 3.5 fold difference in K_d and K_o from latitude 40–50°S' alone, but also that $\bar{E}_o$ in the mixed layer can vary by a factor of 11 (Fig. 4). Thus the productivity of oceanic phytoplankton in New Zealand's EEZ may be expected to vary more than predicted by Vincent, Wake et al. (1989). An improved understanding of the factors controlling spatial variability in phytoplankton productivity and biomass in New Zealand's EEZ is a major goal for future research.

ACKNOWLEDGMENTS

We thank Anthony Cole, Stuart Pickmere, Julie Hall, and Lynelle May for assistance on the ship. Shaun Falconer and Anne-Maree Schwarz collated and processed the optical data set. The study was funded by the Foundation for Research, Science and Technology under contract No. CO1214 and CO1304. The manuscript was typed by Carol Whaitiri with figures by Peter Bennett. Dr John T. O. Kirk provided useful comments on a draft of this paper, which was further improved following referee comment by Dr J. Priddle and Dr S. Sathyandranath.

REFERENCES

Bricaud, A.; Morel, A.; Prieur 1981: Absorption by dissolved organic mater of the sea (yellow substance) in the UV and visible domains. *Limnology and oceanography 26*: 43–53.

Bricaud, A.; Stramski, D. 1990: Spectral absorption coefficients of living phytoplankton and nonalgal biogenous matter: A comparison between the Peru upwelling and the Sargasso Sea. *Limnology and oceanography 35*: 562–582.

Davies-Colley, R. J. 1992: Yellow substance in coastal and marine waters round the South Island, New Zealand. *New Zealand journal of marine and freshwater research 26*: 311–322.

Fenton, N.; Priddle, J.; Tett, P. 1994: Regional variations in bio-optical properties of the surface waters in the Southern Ocean. *Antarctic science 6*: 443–448.

Heath, R. A. 1976: Models of the diffusive-advective balance at the subtropical convergence. *Deep-sea research 23*: 1153–1164.

Heath, R. A. 1985: A review of the physical oceanography of the seas around New Zealand. *New Zealand journal of marine and freshwater research 19*: 79–124.

Hoepffner, N.; Sathyendranath, S. 1992: Bio-optical characteristics of coastal waters: absorption spectra of phytoplankton and pigment distribution in the western North Atlantic. *Limnology and oceanography 37*: 1660–1679.

Jerlov, N. G. 1951: Optical studies of ocean water. *Report of the Swedish deep-sea expedition 3*: 1–59.

Jerlov, N. G. 1976: Marine optics. *Elsevier oceanography series 14*. 231 p.

Kirk, J. T. O. 1981: Monte Carlo study of the nature of the underwater light field in, and the relationships between, optical properties of turbid yellow waters. *Australian journal of marine and freshwater research 32*: 517–532.

Kirk, J. T. O. 1994: Light and photosynthesis in aquatic ecosystems. 2nd edition. Cambridge University Press. 509 p.

Kumar, S. K.; Vincent, W. F.; Austin, P. C.; Wake, G. C. 1991: Picoplankton and marine food chain dynamics in a variable mixed layer: a reaction diffusion model. *Ecological modelling 57*: 193–219.

McBride, G. 1992: Simple calculation of daily photosynthesis by means of five photosynthesis-light equations. *Limnology and oceanography 37*: 1796–1808.

Pelevin, V. N.; Rutkovskaya, V. A. 1977: On the optical classification of ocean waters from the spectral attenuation of solar radiation. *Oceanology 17*: 287–232.

Prieur, L.; Sathyendranath, S. 1981: An optical classification of coastal and oceanic waters based on the specific spectral absorption curves of phytoplankton pigments, dissolved organic matter and other particulate materials. *Limnology and oceanography 26*: 671–689.

Singleton, R. J. 1995: Hydrological data from research voyage 3024, February-March 1995. *New Zealand Oceanographic Institute, Biology Section report 95–1*. 73 p.

Smith, R. C.; Baker, K. S. 1978: Optical classification of natural waters. *Limnology and oceanography 23*: 260–267.

Smith, R. C.; Baker, K. S. 1981: Optical properties of the clearest natural waters (200–800 nm). *Applied optics 20*: 177–184.

Strickland, J. D. H.; Parsons, T. R. 1972: A practical handbook of seawater analysis (2nd edition). *Bulletin 167*, Fisheries Research Board of Canada.

Sullivan, C. W.; Arrigo, K. R.; McClain, C. R.; Comiso, J. C.; Firestone, J. 1993: Distributions of phytoplankton blooms in the Southern Ocean. *Science 262*: 1832–1837.

Topliss, B. J.; Miller, J. R.; Horne, E. P. W. 1989: Ocean optical measurements. II. Statistical analysis of data from Canadian eastern arctic waters. *Continental shelf research 9*: 135–152.

Vincent, W. F. 1983: Phytoplankton production and winter mixing: contrasting effects in two oligotrophic lakes. *Journal of ecology 71*: 1–20.

Vincent, W. F.; Chang, F. H.; Cole, A.; Downes, M. T.; James, M. R.; May, L.; Moore, M.; Woods, P. M. 1989: Short-term changes in planktonic community structure and nitrogen transfers in a coastal upwelling system. *Estuarine, coastal and shelf science 29*: 131–150.

Vincent, W. F.; Howard-Williams, C.; Tildesley, P.; Butler, E. 1991: Distribution and biological properties of oceanic water masses around the South Island, New Zealand. *New Zealand journal of marine and freshwater research 25*: 21–42.

Vincent, W. F.; Wake, G. C.; Austin, P. C.; Bradford, J. M. 1989: Modelling the upper limit to oceanic phytoplankton production as a function of latitude in the New Zealand Exclusive Economic Zone. *New Zealand journal of marine and freshwater research 23*: 401–410.

Viner, A. B. 1990: Dark ^{14}C uptake, and its relationships to nitrification and primary production estimates in a New Zealand upwelling region. *New Zealand journal of marine and freshwater research 24*: 221–228.

Walker, P. M.; Trexler, C. T. 1977: Low sun angle photography. *Photogrammetric engineering and remote sensing 43*.